Intra- and Intermolecular π-Type Hydrogen Bonding in Aryl Alcohols: UV and IR−UV Ion Dip Spectroscopy

Michel Mons,[†] Evan G. Robertson,[‡] and John P. Simons*

Physical and Theoretical Chemistry Laboratory, Oxford University, South Parks Road, Oxford, OX1 3QZ, United Kingdom, and Service des Photons, Atomes et Molecules, Commissariat a l'Energie Atomique, CEN Saclay, 91191 Gif-sur-Yvette Cedex, France

Received: September 9, 1999

The structures of benzyl alcohol, its 1:1 water complex, and its dimer have been investigated by R2PI spectroscopy and IR−UV ion dip spectroscopy, combined with ab initio computation. The sole molecular conformer observed in the jet has a gauche arrangement of the gauche arrangement of the OH group relative to the C_1-C_α bond, but the extent of π-type intramolecular H-bonding is small. Analysis of its rotational band contours suggests the incidence of vibronic coupling involving motion of the side chain and also leads to an estimate for the dihedral angle τ_1(OCCC) lying in the range 35°−60°, in good agreement with the values (50°−60°) indicated by high-level ab initio calculations. The 1:1 water complex is assigned to a structure in which water binds as a proton acceptor to the alcohol group, and as a weak proton donor to the π-system of the aromatic ring. The arrangement of H-bonds is similar within the dimer: the OH of one molecule acts as both acceptor to the alcohol group and as donor to the π-system of the other molecule. Reexamination of published UV band contour and IR/UV ion dip spectroscopic data on 3-phenylpropanol provides unambiguous assignments for the two conformers most heavily populated in the jet expansion: they have AGt and GGt conformations about their $C_\alpha-C_\beta$ (anti/gauche), $C_\beta-C_\gamma$ (anti/gauche), and $C_\gamma-O$ (trans/gauche) bonds that do not involve any OH···π bond. The consequences of increasing chain length for the formation of OH···π bonds is discussed with reference to benzyl alcohol, 2-phenylethanol, and 3-phenylpropanol. The short side-chain of benzyl alcohol permits only a very weak OH···π interaction. The extra methylene units of 2-phenylethanol and 3-phenylpropanol provide enough flexibility for significant OH···π interactions to be possible, but only in 2-phenylethanol does this lead to a strong energetic preference for the H-bonded conformer: the interaction energy gained via the intramolecular H-bond in 3-phenylpropanol is negated by the strain induced in the aliphatic chain.

1. Introduction

The conformational properties of aryl alcohols, and especially benzyl alcohol, have been the subject of numerous spectroscopic investigations.[1−12] The extent to which a flexible side chain allows the possibility of OH···π type intramolecular hydrogen bonding has been of particular interest.

A UV band contour study of 3-phenylpropanol (PPAL), conducted in this laboratory,[1] led to partial assignments of conformers in the jet expansion. The strongest feature in the $S_1 \leftarrow S_0$ spectrum was associated with conformer GGt (or GGg) in Figure 1, and the next strongest to conformer AGt (or AGg). An independent IR−UV ion dip study by Mikami's group[2] probing the OH stretch region concluded that at least six conformers were present in the jet and one of the weaker features was assigned to conformer GG′g-π with an OH···π interaction (see Figure 1).

2-Phenylethanol (PEAL), with only two methylenes in the side chain, has also been studied in this laboratory, first by UV band contour analysis[3] and second using UV−UV and IR−UV ion dip techniques.[4] In the first study, the five main features observed in the region of the band origin were assigned to the conformers of the molecule indicated by ab initio calculation, three gauche and two anti (about OCCC) with some doubt about the assignment of the weak fifth band. Subsequent UV−UV hole-burning experiments, however, established that only *two* conformers were present in the jet.[4] IR−UV ion dip data, in combination with the band contour analysis, allowed an unambiguous assignment of the heavily populated species to conformer Gg-π and the remaining one to conformer At, shown in Figure 2. Concurrent with the second study, a parallel IR−UV investigation of PEAL was carried out in another laboratory.[2] The authors of that study also concluded that the two strongest features in the electronic spectrum were associated with just one molecular conformer, on the basis of identical OH stretch frequencies. Their assignment of the heavily populated conformer to a non-H-bonded form, however, was inconsistent with its red-shifted OH stretch frequency and the results of high-level ab initio calculations.[3,4] An analysis of the UV band contours of tyrosol, the para-substituted analogue of PEAL, reveals a pattern similar to PEAL: two highly populated Gg-π conformers and an At conformer are present in the jet.[5] Finally, the two most prominent 1:1 hydrates of PEAL formed in the jet expansion have been assigned by examination of their UV band contours[6] and their OH stretch frequencies measured by IR−UV ion dip spectroscopy.[4] In one, water binds as a

* Corresponding author. Fax: 44 1865 275410. E-mail: jpsimons@physchem.ox.ac.uk.
[†] Commissariat a l'Energie Atomique, CEN Saclay. Fax: 33 169 088707. E-mail: mmons@cea.fr.
[‡] Fax: 44 1865 275410. E-mail: evanrob@physchem.ox.ac.uk.

10.1021/jp993178k CCC: $19.00
Published on Web 01/22/2000

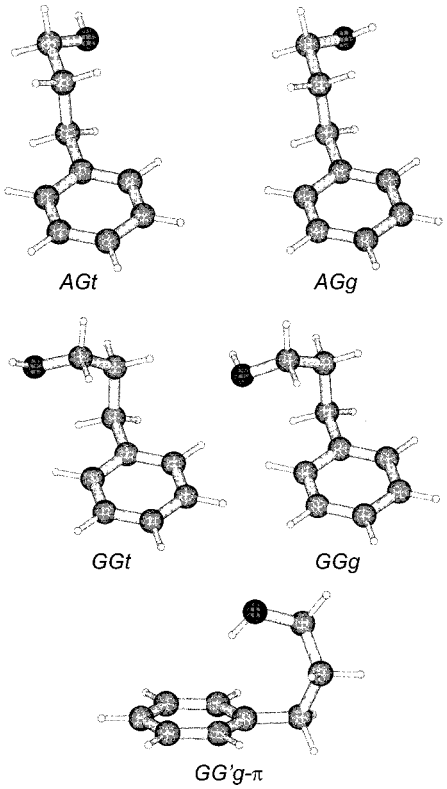

Figure 1. Conformational structures of 3-phenylpropanol,[1] labeled according to the arrangement of the side chain with respect to $C_{ipso}C_\alpha C_\beta C_\gamma$ (gauche/anti), $C_\alpha C_\beta C_\gamma O$ (gauche/anti) and CCOH (gauche/trans), with a π label for the complex exhibiting an intramolecular H-bond.

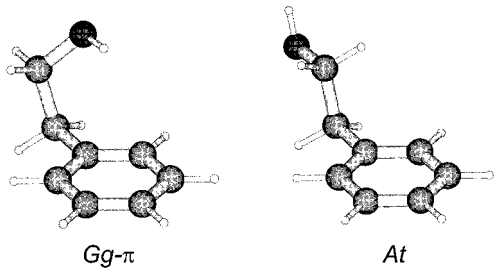

Figure 2. Conformers of 2-phenylethanol observed in the jet expansion,[4] labeled according to the arrangement of the side chain with respect to CCCO (gauche/anti) and CCOH (gauche/trans), with a π label for the complex exhibiting an intramolecular H-bond.

proton acceptor to the alcohol group and as a proton donor to the π system of the ring. In the other, water acts as a proton acceptor to the alcohol group and is further stabilized by a weak van der Waals interaction, $O\cdots HC_{ring}$.

The conformation of benzyl alcohol (BA) may be defined by two dihedral angles of the side chain, τ_1(OCCC) and τ_2(HOCC). IR[7] and NMR[8,9] studies of BA in condensed phase generally conclude that the predominant component has a gauche conformation about τ_2(HOCC), with some indication of a minor component with τ_2(HOCC) = 180°. The lack of consensus concerning conformation about τ_1(OCCC), however, is a common introductory theme in a series of experimental investigations.[2,7,8,10] The latest of many condensed phase IR studies[7] suggests that at least two conformers are present, defined by τ_1(OCCC) = 0° (planar) and 60°, but a third conformation, with τ_1(OCCC) = 90° could not be ruled out. The most recent NMR study of BA[8] found proton−proton coupling constants broadly consistent with a rather low-level ab initio (STO-3G) potential energy surface, in which the global minimum corresponded to τ_1(OCCC) = 43°. In the molecular structure determined by gas-phase electron diffraction,[11] τ_1(OCCC) is 54° (and τ_2(HOCC) is either +60° or −60°). In a detailed examination of the electronic spectroscopy of BA,[10] evidence was found for only one conformer in the supersonic jet; analysis of low-frequency torsional progressions and the number of observed conformers in a series of structural analogues led to the assignment of BA to a single structure with τ_1(OCCC) = 90°. Very recently, the IR−UV ion dip spectroscopic study of BA by Mikami's group[2] led to the assignment of *two* conformers through comparison with ab initio calculations at the HF/6-31G level. The dominant feature in the electronic spectrum, with an OH stretch frequency of 3650 cm^{-1}, was assigned to a planar conformer with τ_1(OCCC) ≈ 0° and τ_2(HOCC) ≈ 0°, while a much weaker feature, with a red-shifted OH stretch frequency of 3585 cm^{-1}, was assigned to a structure similar to conformer *g* in Figure 3. The large red shift was attributed to a strong $OH\cdots\pi$ interaction in the molecule, a finding which is surprising given that the species responsible is barely populated in the jet. While BA might display varying behavior in solution phase, depending on solvent and concentration, it is clear that the gas-phase studies of BA should converge on the unique structure corresponding to the global potential minimum. An additional R2PI investigation of dissociative and reactive fragmentation in ionized clusters of BA with water and ammonia has also been reported.[12]

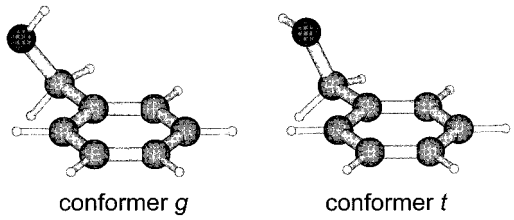

Figure 3. Conformers of benzyl alcohol predicted by MP2/6-31+G** calculations with their relative energies, see Table 1. The labeling (g/t) refers to a gauche or trans conformation about the CO bond.

Mass-selected IR−UV ion dip spectroscopy is a technique well suited to diagnosing hydrogen bonds because it allows the separate measurement of vibrational spectra for each species present in a jet expansion.[13−17] The sensitivity of the OH/NH stretch frequencies to both side chain conformation and to the extent of intra- and intermolecular hydrogen bonding has been particularly valuable in studies of a range of flexible aromatic alcohols and amines and their hydrated complexes.[2,4,18] In this work, the IR−UV spectroscopy of BA is reexamined, and new UV band contour data are also presented and analyzed. The result is a coherent picture that is consistent with all the gas-phase data and with the results of high-level ab initio calculations. In addition, the structures of the 1:1 complex of BA and its dimer have been assigned, and the strength of H-bonded interactions has been examined through IR−UV data.

2. Methodology

The mass-selected resonant two-photon ionization (R2PI) system has already been described elsewhere.[3] Briefly, the jet of BA molecules or complexes was generated by a pulsed valve operating at a moderate temperature (65 °C) under a typical He stagnation pressure of 3 bar, and with a room temperature partial pressure of water when hydrated complexes were studied. The jet was skimmed before entering the interaction region of a differentially pumped time-of-flight mass spectrometer. The ionizing laser (frequency-doubled Lambda Physik FL2002 dye laser, pumped by a Nd:YAG laser) was focused onto the jet at

TABLE 1: Properties of Benzyl Alcohol Conformers, Calculated at the HF/6-31+G, B3LYP/6-31+G*, and MP2/6-31+G** Levels**

	conformer g			conformer t		
level	HF	B3LYP	MP2	HF	B3LYP	MP2
E_{rel}/kJ mol^{-1}	0.0	0.0	0.0	4.5	5.5	4.5
E_{rel} + zp/kJ mol^{-1} [a]	0.0	0.0	0.0	3.5	4.6	3.6
τ_1(OCCC)/deg	43.5	54.3	56.9	12.0	25.1	72.8
τ_2(HOCC)/deg	58.9	54.9	54.4	175.6	172.5	177.9
$\tau_1 = 0°$ barrier/cm^{-1}	335	397	531			242
$\tau_1 = 90°$ barrier/cm^{-1}	280	182	179			1.5
A/MHz	4886.2	4745.8	4704.2	5007.6	4833.7	4665.8
B/MHz	1480.6	1455.3	1471.0	1499.0	1468.2	1478.7
C/MHz	1183.0	1177.1	1191.8	1164.2	1168.0	1213.2

[a] Zero-point corrections at the HF level were scaled by 0.9. The B3LYP zero-point correction was used for both the B3LYP and MP2 relative energies.

a point ~60 mm downstream of the nozzle and the gated ion signal was averaged and recorded through a PC-controlled Tektronix digital oscilloscope. An intracavity Etalon was used to narrow the laser line width when band contours were recorded.

IR−UV ion dip spectra were recorded with the Lambda Physik FL2002 laser as probe, successively tuned to the $S_1 \leftarrow S_0$ spectral feature of interest. The IR radiation (ca. 2.8 μm) was generated by a Continuum difference frequency generation module at the output of a Nd:YAG-pumped Continuum ND6000 dye laser, operating with the LD765 dye. The IR beam (bandwidth 1 cm^{-1}) had a typical energy of 1 mJ per pulse and was mildly focused onto the jet antiparallel to the UV probe laser. The delay between the IR and UV lasers was ~100 ns, which restricted the IR depletion to the ground state of the probed species only.

Ab initio calculations on BA and its complexes were performed using the Gaussian 94 suite of programs[19] in order to aid experimental interpretation. The BA monomer was studied via full geometry optimizations at the HF/6-31+G**, MP2/6-31+G**, and B3LYP/6-31+G* levels of theory. Barriers to rotation about the $C_{ipso}C_\alpha$ bond were calculated by performing a series of optimizations in which the dihedral angle τ_1(OCCC) was constrained to values in the range 0°−90°. The structure of possible 1:1 water clusters was investigated at the MP2/6-31G* level, with water bound to each of the three possible binding sites of the alcohol group. Vibrational frequencies of the monomer and the 1:1 water complexes were computed at the B3LYP/6-31+G* level, which has been found to give good OH frequencies for systems which include π H-bonding where dispersion is important. Calculations of the BA dimer were restricted to the HF/6-31G* level because of the large number of atoms involved.

3. Results

3.1. Ab Initio Results on Benzyl Alcohol. Ab initio calculations on benzyl alcohol (BA) indicated two minima in the potential energy surface at each level of theory employed, one with a gauche and the other with a trans arrangement of the HOCC side chain: the MP2/6-31+G** structures are shown in Figure 3 and the data are summarized in Table 1. Conformer g is energetically favored by a similar margin at each level of theory, ca. 4 kJ mol^{-1}. On the important question of conformation about the OCCC bond, the calculations agree that the most stable conformer has a gauche configuration, with dihedral angles τ_1(OCCC) of 45°, 54°, and 57°, respectively, for the HF, DFT, and MP2 calculations. Barriers to rotation about the $C_{ipso}-C_\alpha$ bond are greater at 0° (335, 397, and 531 cm^{-1}) than at 90° (280, 182, and 179 cm^{-1}). The results for the trans conformer vary more with the level of theory: dihedral angles about the OCCC bond are found to be 12°, 25°, and 73°, respectively. At the highest level of theory, MP2/6-31+G**, the barrier is less than 2 cm^{-1} when τ_1(OCCC) = 90° and 242 cm^{-1} at τ_1(OCCC) = 0°. A preference for τ_1(OCCC) ≈ 90° in conformer t parallels the conclusions of a microwave spectroscopic study on the isoelectronic molecule benzyl fluoride[20] that the fcc plane is orthogonal to the ring.

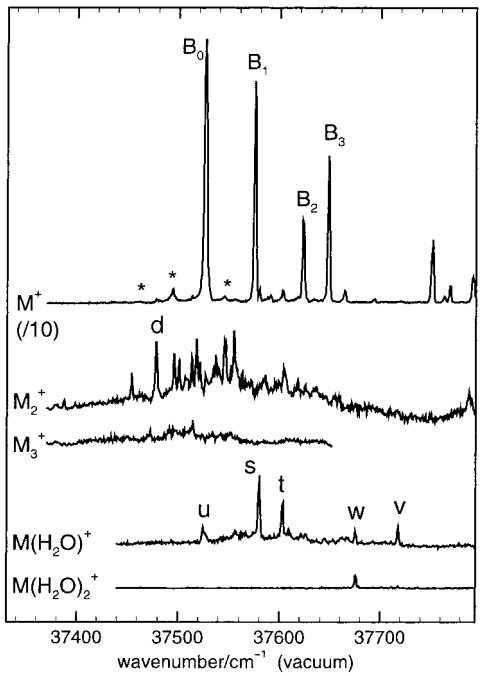

Figure 4. Mass-selected R2PI spectroscopy of benzyl alcohol and associated clusters. The peaks marked with an asterisk appear with much greater intensity in a warm expansion. The water complex bands are labeled in accord with an earlier study.[12]

3.2. R2PI Spectroscopy of Benzyl Alcohol. The mass-selected R2PI spectrum of the BA molecule in the region of its $S_1 \leftarrow S_0$ band origin is shown in Figure 4. The dominant peaks in the monomer mass channel, labeled B_0-B_3, have been assigned previously to a single conformer on the basis of isotope shifts.[10] Some of the weaker features, marked with an asterisk, appear with much greater intensity in the warmer expansion conditions encountered when only a small delay, between the nozzle opening and the arrival of the laser pulse, is used. In the earlier R2PI study by Bernstein's group,[10] they were assigned to hot bands, originating from low-frequency torsional excitation in the ground electronic state.

Band contours of the $S_1 \leftarrow S_0$ origin, B_0, and the first vibronic feature, B_1, are shown in the upper traces of Figure 5. A cross-correlation fitting procedure (described elsewhere[1,5]) was used to generate the simulated contours in the lower traces. The resulting rotational constants and a:b:c-type hybrid band characters are given in Table 2. The spacing of the Q-subband heads in the contour of B_0 allows a good evaluation of $(A-\bar{B})''$. The value obtained, 0.1151 ± 0.0020 cm^{-1}, is closer to the MP2 prediction for conformer g (0.1125 cm^{-1}) than conformer t (0.1107 cm^{-1}). In practice, this says more about the position of the oxygen than it does about the alcohol hydrogen, since the $(A-\bar{B})''$ parameter is insensitive to the position of the light hydrogen nucleus.

The same rotational constants were used to simulate bands B_0 and B_1, but very different hybridization parameters were required (8:72:20 and 62:27:11, respectively). The hybrid

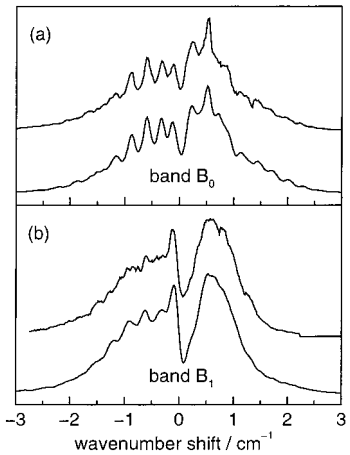

Figure 5. Experimental and simulated rotational contours for bands B_0 (a) and B_1 (b) of benzyl alcohol. Upper traces: experimental R2PI spectra. Lower traces: optimized simulations using the data from Table 2, $T_{rot} = 3.7$ K (a), 5.8 K (b) and laser line width = 0.12 cm^{-1}.

TABLE 2: Fitted Molecular Parameters and ab Initio Predictions for Benzyl Alcohol

species	$(A-\bar{B})''$/cm^{-1}	$\bar{B}''$/cm^{-1}	$(B-C)''$/cm^{-1}	$\mu_a^2:\mu_b^2:\mu_c^2$
band B_1	0.1151	0.0403	0.0081	8:72:20
band B_2	0.1151[a]	0.0403[a]	0.0081[a]	62:27:11
conf t[b]	0.1107	0.0449	0.0089	
conf g (57°)[b]	0.1125	0.0444	0.0093	
conf g (0°)[c]	0.1197	0.0436	0.0109	
conf g (15°)[c]	0.1187	0.0438	0.0108	
conf g (30°)[c]	0.1171	0.0440	0.0105	
conf g (45°)[c]	0.1147	0.0442	0.0099	
conf g (60°)[c]	0.1119	0.0445	0.0092	
conf g (75°)[c]	0.1099	0.0446	0.0086	
conf g (90°)[c]	0.1097	0.0446	0.0085	

[a] S_0 rotational constants for band B_1 were constrained to the fitted values from band B_0. [b] Full MP2/6-31+G** optimizations. [c] MP2/6-31+G** optimizations subject to the constraint of a fixed dihedral angle τ_1(OCCC).

characters of the two bands suggest that their transition moment alignments differ by ca. 36°. A very similar phenomenon was also observed in the Gg-π conformer of 2-phenylethanol (PEAL): while the origin band is b-type, exciting one quantum of a low-frequency vibration in S_1 gives rise to a band contour with a large a-type component.[4] This was tentatively ascribed to vibronic coupling to another excited electronic state, in a fashion similar to that observed in phenylacetylene.[21] In both PEAL and BA, the vibrational mode excited in S_1 involves torsion about the $C_{ipso}-C_\alpha$ bond, so it is likely that the same mechanism is responsible in both molecules.

3.3. IR/UV Spectroscopy of Benzyl Alcohol. The ion dip IR spectrum recorded with the probe laser centered on the origin band B_0 is shown in Figure 6a, together with the corresponding IR spectra of the two observed conformers of PEAL, for comparison. The OH stretch band of BA (3649 cm^{-1}) lies closer to the frequency of the H-bonded Gg-π conformer of PEAL than the all-trans At conformer, suggesting its association with a gauche HOCC side chain conformation. Conformer t of BA might be expected to have a very similar OH frequency to the At conformer of PEAL (3678 cm^{-1}) or trans ethanol (3676 cm^{-1}).[23] The OH stretch frequency of BA conformer g, on the other hand, might be expected to lie around 3660 cm^{-1} (the value for gauche ethanol), if there is no H-bonding interaction. The position at 3649 cm^{-1} indicates a very weak H-bond interaction, which induces a red shift of ca. 11 cm^{-1}, much less than the 36 cm^{-1} red shift seen in the Gg-π conformer of PEAL.

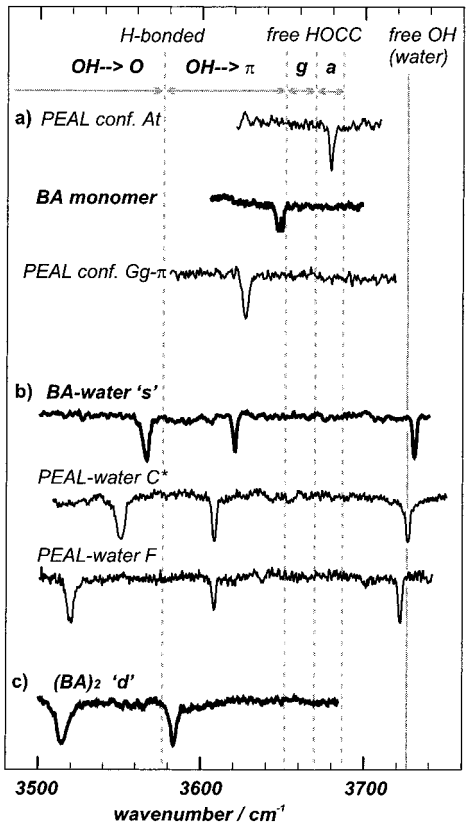

Figure 6. IR ion dip spectra probing (a) band B_0 in mass channel BA^+, (b) band s in mass channel BA^+−water, and (c) band d in mass channel $(BA)_2^+$. The shape of the BA band in (a) is affected by a dip in laser power at 3649.3 cm^{-1}, caused by a strong absorption band of atmospheric water.[22] For the sake of comparison, spectra are also displayed for 2-phenylethanol (a) and its 1:1 hydrates (b).

TABLE 3: Experimental and Calculated OH Stretch Frequencies for Conformers of BA and Its Complexes[a]

exptl UV band probed	freq/ cm^{-1}	ab initio species	mode descripn	freq/ cm^{-1}	intensity/ km mol^{-1}
monomer B_0	3649	conf g	OH_{BA}	3648[b]	18
		conf t	OH_{BA}	3676[b]	28
BA−water s	3566	BA−water **I**	$OH_{BA} \rightarrow O_{water}$	3526[b]	270
	3621		$OH_{water} \rightarrow$ p	3634[b]	29
	3731		free OH_{water}	3755[b]	98
		BA−water **II**	$OH_{water} \rightarrow O_{BA}$	3492[b]	378
			OH_{BA}	3650[b]	26
			free OH_{water}	3734[b]	87
		BA−water **III**	$OH_{water} \rightarrow O_{BA}$	3508[b]	591
			OH_{BA}	3648[b]	28
			free OH_{water}	3728[b]	121
$(BA)_2$ d	3515	$(BA)_2$ **1**	$OH_{BA} \rightarrow O_{BA}$	3538[c]	301
	3584		$OH_{BA} \rightarrow \pi$	3590[c]	83
		$(BA)_2$ **2**	$OH_{BA} \rightarrow O_{BA}$	3544[c]	320
			$OH_{BA} \rightarrow \pi$	3588[c]	93

[a] Experimental precision is estimated to be 2 cm^{-1}. [b] B3LYP/6-31+G* calculations. The scaling factor, 0.9763, has been determined using the OH stretches of the two observed PEAL conformers (Gg-π and At) [4] as a benchmark. [c] HF/6-31G* calculations. The scaling factor, 0.879, has been determined using the $OH_{phenol} \rightarrow O_{water}$ mode of the phenol−water complex[16] as a benchmark.

This analysis is confirmed by comparison with ab initio calculations at the B3LYP/6-31+G* level; see Table 3. The predicted OH stretch frequency for BA conformer t is 3676 cm^{-1}, but for conformer g it is 3648 cm^{-1}, in excellent agreement with the observed frequency, 3649 cm^{-1}.

3.4. Conformation of the Benzyl Alcohol Side Chain. Having established by IR /UV spectroscopy that the HOCC bond

of BA has a gauche conformation, it is worth reexamining the electronic spectra to quantify τ_1, the dihedral angle about the OCCC bond. The most pertinent information is the value of the $(A-\bar{B})''$ parameter obtained from the band contour, 0.1151 $\pm$ 0.0020 cm^{-1}. MP2/6-31+G** optimizations of gauche benzyl alcohol with τ_1(OCCC) fixed at 0°, 15°, 30°, 45°, 60°, 75°, and 90° lead to the predictions for $(A-\bar{B})''$ given in Table 2. To test the quality of these predictions, calculations were performed at the same level of theory on the closely related molecule, ethylbenzene. The resulting rotational constants are very close to the experimental values from microwave spectroscopy,[24,25] but the $(A-\bar{B})''$ parameter is underpredicted by 0.0009 cm^{-1}. Taking this into account, consideration of the data in Table 2 suggests that the dihedral angle τ_1(OCCC) lies in the range 35°−60°. The observed conformer is certainly not planar, but the results also suggest that the CO side chain is not perpendicular to the ring either. A more precise estimate would require accurate measurement of the rotational constants by high-resolution electronic or microwave spectroscopy, preferably with isotopic substitution.

In the earlier R2PI study, bands B_1 and B_2, blue-shifted from the origin (37 526.5 cm^{-1}) by 50 and 96 cm^{-1}, were associated with vibronic transitions exciting a low-frequency torsion mode in the side chain.[10] Assuming a perpendicular side chain geometry, τ_1(OCCC) = 90°, they were assigned as T_0^2 and T_0^4, since the $\Delta v_\tau = \pm 1, \pm 3$ torsional transitions would be forbidden by symmetry. The bands red-shifted by 32 and 64 cm^{-1} from the origin were assigned to the transitions T_2^0 and T_4^0, using similar arguments. The present results, which imply that the side chain is *not* perpendicular to the ring plane, bring this interpretation into question. The observation of two hot bands, at positions −32 and +18 cm^{-1} relative to the origin, suggests that they do share a common S_0 vibrational level at 32 cm^{-1}, since the spacing is the same as between B_0 and B_1 (50 cm^{-1}). There is also supporting evidence from the matrix Raman spectrum of BA suggesting the presence of S_0 vibrational levels at 32 and 63 cm^{-1}.[26] If they are assigned to 2 and 4 quanta of torsion, however, an additional $S_1 \leftarrow S_0$ band is expected with a shift very close to +9 cm^{-1}, corresponding to T_1^1. It should be even stronger than the other hot bands, since the $v_\tau = 1$ state would be more populated. The absence of such a band argues instead that the hot bands at −32 and −64 cm^{-1} be assigned to transitions T_1^0 and T_2^0, and bands B_1 and B_2 to transitions T_0^1 and T_0^2. The purely *harmonic* ground state vibrational frequency, predicted from the ab initio calculations of the conformer g at the DFT/B3LYP level, is 36 cm^{-1}.

To summarize, high-level ab initio calculations suggest *the most stable conformer of BA has a gauche arrangement of the HOCC atoms and that the dihedral angle τ_1(OCCC) is ca. 50°−60°, with nonnegligible barriers at 0° and 90°*. Such a structure is consistent with all our experimental data on the observed conformer: the OH stretch frequency (3649 cm^{-1}), the $(A-\bar{B})''$ parameter (0.1151 $\pm$ 0.0020 cm^{-1}), and the appearance of hot bands in the electronic spectrum suggesting a low-frequency S_0 vibrational mode around 32 cm^{-1}. In light of this analysis, the gas-phase electron diffraction determination that τ_1(OCCC) $\approx$ 54°[11] should be regarded as reliable and the most accurate experimental measurement to date.

3.5. The 1:1 Water Complex of Benzyl Alcohol. The labeled features in the $M(H_2O)^+$ mass channel of Figure 4 were assigned to clusters with one (s,t), two (u), three (v), and four (w) water molecules by Bernstein et al.[12] on the basis of pulsed nozzle/laser timing delay studies. The IR−UV ion dip spectrum obtained with the probe laser centered on the water complex band "s" is shown in Figure 6b; an identical spectrum was also obtained by probing band "t", suggesting that s and t are separate vibronic transitions of one complex. The observation of three distinct bands in its OH stretch region confirms its association with a 1:1 water complex, and comparison with other systems[4,14−16] indicate the following assignments: OH → O (3566 cm^{-1}), OH → π (3621 cm^{-1}), and free OH_{water} (3731 cm^{-1}). Since the OH group of BA only forms a very weak π-type H-bond, the red-shifted band at 3621 cm^{-1} suggests the proton donor to the π system of the ring is the bound water molecule, in agreement with the most stable ab initio predicted structure, complex **I**, shown in Figure 7a. The equivalent water complex **I** in PEAL (Figure 7b) gives rise to the spectrum labeled PEAL-water C* in Figure 6b, which is very similar. (The third spectrum in Figure 6b, labeled PEAL-water F, is associated with the alternative 1:1 complex **II** of PEAL shown in Figure 7b, [4] which resembles the BA−water complex **II**.)

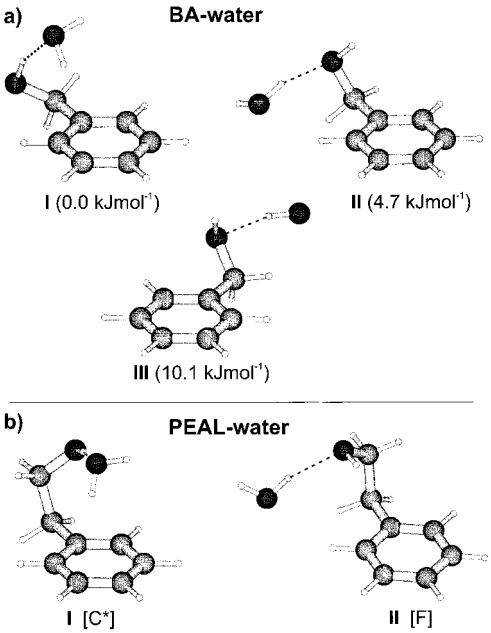

Figure 7. Ab initio (MP2/6-31G*) structures for 1:1 hydrates of benzyl alcohol (a) and 2-phenylethanol (b). The relative energies for the BA−water complexes, shown in parentheses, were computed at the MP2/6-31G* level and include zero-point corrections (B3LYP/6-31+G*). Assignments of PEAL complexes **I** and **II**[4] are indicated in (b).

This assignment to structure **I** is supported by a close examination of the ab initio results. The structures in Figure 7a, with water bound to each of the three possible binding sites of the alcohol group, result from MP2-6-31G* level calculations. (In cases where a slightly different alternative structure was possible, which varied only in the orientation of the nonbonded hydrogen of water, the more stable variant is shown.) The calculated relative energies favor complex **I** over **II** by 4.7 kJ mol^{-1} and **II** over **III** by a further 5.4 kJ mol^{-1}. OH stretch frequencies for these three complexes, calculated at the B3LYP/6-31+G* level, are given in Table 3. A critical difference is found in the assignment of the OH stretch mode with intermediate frequency. In complexes **II** and **III**, it is the OH_{BA} oscillator, calculated to occur at 3650 and 3648 cm^{-1}. The important fact is that the calculations indicate the OH stretch mode of BA in complexes **II** and **III** is *not* red-shifted, relative to the bare molecule calculation (3648 cm^{-1}), whereas an assignment of the 1:1 complex of BA water to **II** or **III** would imply a red shift of 28 cm^{-1}. In complex **I**, the oscillator with intermediate frequency is the $OH_{water} \rightarrow \pi$ oscillator with a calculated frequency of 3634 cm^{-1}, in good agreement with the observed

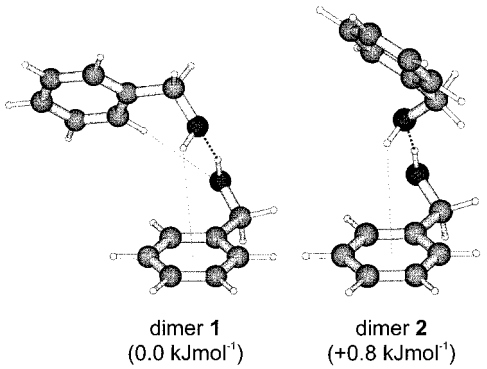

Figure 8. Ab initio (HF/6-31G*) structures for the benzyl alcohol dimer. Relative energies, including zero-point corrections, are shown in parentheses.

band at 3621 cm^{-1}. If the free OH_{water}, $OH_{water} \rightarrow \pi$, and $OH_{molecule} \rightarrow O$ frequencies of BA−water complex **I** are scaled using factors obtained from the very similar PEAL complex **I**,[4] the resulting frequencies (3567, 3624, 3736 cm^{-1}) are very close indeed to the experimental values.

3.6. Benzyl Alcohol Dimer. In the R2PI spectra of Figure 4, a series of bands appear in both the dimer and monomer mass channels, suggesting their association with BA dimer species which partially dissociate. These features were not observed in the spectra reported by Bernstein,[10] but were apparent in the R2PI spectra of Mikami et al.[2] The dimer mass channel was not examined in the latter study, but the peak labeled d was probed by IR/UV ion dip spectroscopy. In the region 3530−3750 cm^{-1}, only one band was evident, which led to the erroneous assignment of d to the gauche monomer of benzyl alcohol. In Figure 6c, our more extended IR/UV ion dip spectrum shows an additional feature at 3515 cm^{-1}, as well as the previously observed band at 3584 cm^{-1}. The large line width of the new feature and its highly red-shifted position are both characteristic of an OH bound to a strong acceptor,[18] which could only be the oxygen of the other BA molecule. Assignment of the 3515 cm^{-1} band to an OH → O oscillator implies that the 3584 cm^{-1} band is associated with a strong OH···π bond, since it is not geometrically possible for both alcohol groups to form OH···O hydrogen bonds. An ab initio study conducted at the HF/6-31G* level found four dimer structures which are consistent with this description. The two most stable are shown in Figure 8. Dimer **1** benefits not only from OH···O and OH···π H-bonds, but also from a weak O···HC_{ring} interaction which could contribute to its slightly greater stability. Vibrational frequency predictions for dimer **1** or dimer **2**, given in Table 3, are both in good agreement with the experimental band positions. The R2PI spectrum in the dimer mass channel includes a number of vibronic progressions, e.g., what appears to be an origin, shifted by −72 cm^{-1} from the monomer band B_0, is accompanied by band d at −48 cm^{-1}, and other bands at −26, −5, and +14 cm^{-1}. The spectrum is too congested for a thorough analysis, but it is quite possible that more than one dimer complex is present in the jet expansion.

4. Discussion

The analysis of the new experimental data reported here for benzyl alcohol and its complexes, together with the reassessment of the earlier corresponding studies of 2-phenylethanol and 3-phenylpropanol, provides a clear and coherent picture of the factors influencing their conformational choice. In particular, comparison of the conformational structures of benzyl alcohol, 2-phenylethanol, and 3-phenylpropanol reveals the way the geometric constraints associated with increasing or decreasing chain length affect the formation of intramolecular OH···π bonds in the bare molecule.

The short side chain of benzyl alcohol prevents the alcohol group from reaching over the ring, and the direction of the HO bond is far from favorable for an OH···π bond. The red shift of approximately 11 cm^{-1} relative to the free OH of a gauche side chain indicates a weak interaction. It is the gauche form that is energetically preferred, by a margin of ca. 4 kJ mol^{-1} according to the high-level theoretical calculations reported here and the analysis of NMR data.[9] It is not clear, however, how much of this energy difference should be attributed to OH···π attraction in conformer g and how much to additional repulsion between the oxygen lone pairs and the π-system in conformer t.

With the addition of an extra methylene group in 2-phenylethanol, the geometry is well suited to forming a π-type H-bond (see Figure 2). The angle between the OH bond and the plane of the ring is still not the optimal 90°, but it is much better than in BA. The experimental H-bond induced red shift of the OH frequency is ca. 36 cm^{-1}, only slightly less than is found in the benzene−methanol complex (42 cm^{-1}).[15] This interaction is sufficient to stabilize the H-bonded Gg-π form by more than 6 kJ mol^{-1} relative to its nearest rival.[3]

Finally, the three methylenes of 3-phenylpropanol do allow the possibility of a π-type H-bond, but only if the dihedral angles of the side chain are far from their optimal values of 60° or 180°. In our earlier LIF/R2PI study of 3-phenylpropanol,[1] band contour analysis combined with ab initio computation permitted assignment of the heavy atom chain conformation for the two strongest features in the electronic spectrum. The position of the alcohol hydrogen could not be determined, of course, as the rotational constants are quite insensitive to it. The strongest feature in the $S_1 \leftarrow S_0$ spectra, at 37 557 cm^{-1}, was assigned either to conformer GGt or GGg (see Figure 1), and the next strongest feature, at 37 591 cm^{-1}, either to conformer AGt or AGg. A recent IR−UV ion dip study of 3-phenylpropanol [2] contains the information needed to complete the picture and distinguish between the alternative g and t conformers. The OH stretch frequencies associated with the two features were found at 3680 and 3682 cm^{-1}, which is very strong evidence for a trans arrangement of the HOCC group. The two most populated conformers in the jet expansion can therefore be identified as the GGt and AGt structures shown in Figure 1. Both have a gauche conformation about the $OC_\gamma C_\beta C_\alpha$ bond, and therefore benefit from a weak van der Waals type interaction O···HC_α. Other weaker spectral features probed in the IR−UV study[2] have OH stretch frequencies of 3630, 3659, and 3662 cm^{-1}. The latter two are clearly associated with a gauche conformation of the HOCC group, but the arrangement of the heavy atoms remains to be determined. The conformer with its OH stretch at 3630 cm^{-1}, the only one assigned in the IR−UV study, has an OH···π bond, consistent with the GG′g-π structure of Figure 1. The observed red shift of ca. 31 cm^{-1} indicates an interaction of reasonable strength, but the energetic cost associated with strain in the chain ($C_1C_\alpha C_\beta C_\gamma = 57°$, $C_\alpha C_\beta C_\gamma O = 79°$, $C_\beta C_\gamma$-OH = 65°, at the MP2/6-31G* level) means that the population of the π H-bonded conformer in the jet is very small.

Analysis of the alcohol conformers actually observed in the jet expansion also reveals something about the relaxation processes. The appearance of multiple conformers with different heavy atom configurations suggests that the barriers to interconversion are sufficiently high to prevent relaxation. For each heavy atom conformation, however, it appears that only one

HOCC conformation is observed, implying that there *is* relaxation about the HO−CC bond. A study which employed microwave spectroscopy to probe conformer populations in pulsed, seeded supersonic expansions concluded that relaxation may occur when barriers to interconversion are 400 cm^{-1} or less.[27] Significant conformational relaxation was seen in ethanol and 2-propanol, but only with carrier gases heavier than helium. The aromatic alcohols apparently show different behavior in this regard.

Figure 6 presents a summary of the OH stretch frequencies of BA and PEAL. The free OH oscillators of trans HOCC and gauche HOCC and of bound water within complexes appear in distinct regions, as do the red-shifted, H-bonded oscillators OH···π and OH···O. Direct comparison of OH stretch frequencies in the complexes of BA and PEAL (Figure 6b,c) reveals clear trends in the H-bond strengths. Both the OH → O and OH → π bands of BA−water are less red-shifted (and therefore the H-bonds are weaker) than in the corresponding PEAL−water C* complex. An examination of MP2/6-31G* geometries shown in Figure 7 suggests a likely reason. The geometry of the Gg-π conformer of PEAL is such that the water molecule in PEAL−water **I** can readily form a π-type H-bond, without straining the $OH_{PEAL}...O_{water}$ H-bond ($\alpha_{OHO} = 172°$). The oxygen of water is situated over the center of the ring, in a manner reminiscent of the benzene−water complex.[14] In contrast, for water to form a π-type H-bond with BA, the $OH_{BA}...O_{water}$ H-bond must be distorted away from linearity ($\alpha_{OHO} = 157°$) and the equilibrium distance ($r_{H...O} = 1.94$ Å) is slightly greater than in PEAL−water **I** ($r_{H...O} = 1.90$ Å), implying a weaker OH···O interaction. In addition, the oxygen of water is not directly over the hexagon defined by the ring carbons in BA, but is displaced sideways, resulting in a weaker OH···π interaction.

A question that arises in considering these water complexes is why two distinct forms are observed in PEAL, but only one in BA. The implication is that the stabilities of the PEAL−water complexes **I** and **II** are much closer than those of their BA−water counterparts. Using simplistic reasoning, both PEAL−water complexes have an OH···O and an OH···π H-bond. The same is true for the BA−water complexes, but the intramolecular π-type H-bond of BA−water complex **II** is very weak, and it does not seem able to compete energetically with BA−water complex **I**.

The geometry of the BA dimer is in some ways analogous to the BA−water complex, but the IR band positions indicate that the bonds formed are even stronger. The red shift for the $OH_{BA} \rightarrow O_{BA}$ oscillator, relative to the monomer OH band, is 133 cm^{-1}, compared to only 82 cm^{-1} for the $OH_{BA} \rightarrow O_{water}$ band of the BA−water complex. This is consistent with the trend for alcohols to act as a stronger H-bond acceptor than a water molecule. In binary clusters with phenol, for example, the red-shift induced when ethanol is the proton acceptor (225 cm^{-1}) [17] is considerably greater than when water is the acceptor (133 cm^{-1}).[16] It is not surprising, therefore, that the frequency of the $OH_{BA} \rightarrow O_{BA}$ oscillator in $(BA)_2$ is close to that of the $OH_{water} \rightarrow O_{PEAL}$ oscillator in PEAL−water F. The red shift for the $OH_{BA} \rightarrow \pi$ oscillator (64 cm^{-1}) is also quite large for a π-type H-bond, in spite of the geometric constraints, which are similar to those affecting the binding of water to BA. In the role of donor to the π system of benzene, alcohols again surpass water. The red shift of the donor OH in the benzene-MeOH complex (42 cm^{-1})[15] is greater than in the benzene−water complex (23 cm^{-1}),[14] for example. The strength of the H-bond interactions can also be related to cooperative effects. In the dimer **1** complex shown in Figure 8, for example, cooperation is enhanced by the fact that each alcohol acts both as a proton donor and as a proton acceptor.

5. Conclusions

Mass-selected R2PI and IR−UV ion dip spectroscopic techniques provide key data for the assignment of molecular conformers and complexes, the interpretation of which is greatly facilitated by high-level ab initio calculations. The data are often complementary; in the present case of aryl alcohols, for example, UV band contours reveal the position of the heavy atoms in the side chain, while the OH stretch frequencies are sensitive to the HOCC conformation. The spectral shifts induced in OH stretch frequencies by H-bonding has helped to reveal the role played by OH···π interactions in determining conformation. In benzyl alcohol, the direction of the HO bond in conformer g permits only a weak OH···π bond and the spectral red shift is very small (≈11 cm^{-1}). The H-bonded conformer g is energetically preferred by a margin of ca. 4 kJ mol^{-1}, but the OH···π interaction does not necessarily account for all of this. Conformer Gg-π of 2-phenylethanol gains the most from the intramolecular H-bond. The H-bond-induced red shift is ca. 36 cm^{-1}, and conformer Gg-π is favored over its nearest rival by more than 6 kJ mol^{-1}. In 3-phenylpropanol, the constraint implied by the three methylene units allow an OH···π bond only if the dihedral angles of the side chain are far from their optimal values of 60° or 180°. A strong interaction is indicated by the induced red shift (ca. 31 cm^{-1}), but the energetic cost associated with distorting the chain means that the π H-bonded conformer is barely populated in the jet. Strain in the chain is a drain on the H-bond gain!

Acknowledgment. The authors gratefully acknowledge the EPSRC for grant support (M.M.) and the Leverhulme Trust for postdoctoral support (E.G.R.). We also thank the Laser Support Facility at the Rutherford Appleton Laboratory for the loan of the IR laser system and especially Dr. M. Towrie for his assistance.

References and Notes

(1) Elks, J. M. F.; Robertson, E. G.; Simons, J. P.; McCombie, J.; Walker, M. *Phys. Chem. Commun*. **1998**, *3*.
(2) Guchhait, N.; Ebata, T.; Mikami, N. *J. Am. Chem. Soc*. **1999**, *121*, 5705−5711.
(3) Dickinson, J. A.; Hockridge, M. R.; Kroemer, R. T.; Robertson, E. G.; Simons, J. P.; McCombie, J.; Walker, M. *J. Am. Chem. Soc*. **1998**, *120*, 2622−2632.
(4) Mons, M.; Robertson, E. G.; Snoek, L. C.; Simons, J. P. *Chem. Phys. Lett*. **1999**, *310*, 423−432.
(5) Hockridge, M. R.; Knight, S. M.; Robertson, E. G.; Simons, J. P.; McCombie, J.; Walker, M. *PCCP* **1999**, *1*, 407−413.
(6) Hockridge, M. R.; Robertson, E. G. *J. Phys. Chem*. A **1999**, *103*, 3618−3628.
(7) Visser, T.; van der Maas, J. H. *Spectrochim. Acta* **1986**, *42A*, 599−602 and references therein.
(8) Schaefer, T.; Sebastian, R.; Peeling, J.; Penner, G. H.; Koh, K. *Can. J. Chem*. **1989**, *67*, 1015−1021.
(9) Abraham, R. J.; Bakke, J. M. *Tetrahedron* **1978**, *34*, 2947.
(10) Im, H.-S.; Bernstein, E. R.; Secor, H. V.; Seeman, J. I. *J. Am. Chem. Soc*. **1991**, *113*, 4422−4431.
(11) Trætterberg, M.; Østensen, H.; Ragnhild, S. *Acta Chem. Scand. A* **1980**, *34*, 449−454.
(12) Li, S.; Bernstein, E. R. *J. Chem. Phys*. **1992**, *97*, 7383−7391.
(13) Pribble, R. N.; Zwier, T. S. Science **1994**, *265*, 75−79.
(14) Fredericks, S. Y.; Jordan, K. D.; Zwier, T. S. *J. Phys. Chem*. **1996**, *100*, 7810−7821 and references therein.
(15) Pribble, R. N.; Hagemeister, F. C.; Zwier, T. S. *J. Chem. Phys*. **1997**, *106*, 2145−2157.
(16) Mitsuzuka, A.; Fujii, A.; Ebata, T.; Mikami, N. *J. Chem. Phys*. **1996**, *105*, 2618−2627.

(17) Spangenberg, D.; Imhof, P.; Roth, W.; Janzen, Ch.; Kleinermanns, K. *J. Phys. Chem*. A **1999**, *103*, 5918−5924.

(18) Graham, R. G.; Kroemer, R. T.; Mons, M.; Robertson, E. G.; Snoek, L. C.; Simons, J. P., submitted for publication in *J. Phys. Chem. A.*

(19) *Gaussian 94*, Revision C.3; Frisch, M. J.; Trucks, G. W.; Schlegel, H. B.; Gill, P. M. W.; Johnson, B. G.; Robb, M. A.; Cheeseman, J. R.; Keith, T.; Petersson, G. A.; Montgomery, J. A.; Raghavachari, K.; Al-Laham, M. A.; Zakrzewski, V. G.; Ortiz, J. V.; Foresman, B.; Cioslowski, J.; Stefanov, B. B.; Nanayakkara, A.; Challacombe, M.; Peng, C. Y.; Ayala, P. Y.; Chen, W.; Wong, M. W.; Andres, J. L.; Replogle, E. S.; Gomperts, R.; Martin, R. L.; Fox, D. J.; Binkley, J. S.; Defrees, D. J.; Baker, J.; Stewart, J. P.; Head-Gordon, M.; Gonzalez, C.; Pople, J. A. Gaussian, Inc.: Pittsburgh, PA, 1995.

(20) Bohn, R. K.; Sorenson, S. A.; True, N. S.; Brupbacher, T.; Gerry, M. C. L.; Jäger, W. *J. Mol. Spectrosc*. **1997**, *184*, 167−171.

(21) Ribblett, J. W.; Borst, D. R.; Pratt, D. W. *J. Phys. Chem*. A, in press.

(22) Camy-Peyret, C.; Flaud, J. M.; Guelachvili, G.; Amiot, C. *Mol. Phys*. **1973**, *26*, 825−855.

(23) Fang, H. L.; Sworfford, R. L. *Chem. Phys. Lett*. **1984**, *105*, 5−11 and references therein.

(24) MP2/6-31+G** values: $A = 4496.1$, $B = 1471.08$, $C = 1219.5$ MHz. From microwave spectroscopy;[25] $A = 4521.9$, $B = 1468.690$, $C = 1217.049$ MHz.

(25) Caminati, W.; Damiani, D.; Corbelli, G.; Velino, B.; Bock, C. W. *Mol. Phys*. **1991**, *74*, 885−895.

(26) Prystupa, D. A.; Anderson, A.; Torrie, B. H. *J. Raman Spectrosc*. **1994**, *25*, 175−182.

(27) Ruoff, R. S.; Klots, T. D.; Emilsson, T.; Gutowsky, H. S. *J. Chem. Phys*. **1990**, *93*, 3142−3150.